Size-Dependent Photoluminescence from Single Indium Phosphide Nanowires

Mark S. Gudiksen,[†] Jianfang Wang,[†] and Charles M. Lieber*

Department of Chemistry and Chemical Biology, Harvard University,
12 Oxford Street, Cambridge, Massachusetts 02138

Received: December 3, 2001; In Final Form: March 4, 2002

Photoluminescence (PL) imaging and spectroscopy have been used to investigate isolated, individual indium phosphide nanowires (InP NWs) at both room temperature and 7 K. PL images and spectra show that the emission maxima, line shapes, and intensities are nearly identical along the axis of a given NW. PL spectra collected on InP NWs with diameters of 10, 15, 20, and 50 nm show that emission maxima systematically shift to higher energy with decreasing wire diameter, for diameters less than 20 nm. An effective mass model (EMM) has been developed using particle-in-a-cylinder wave functions for electrons and holes to explore quantitatively the diameter-dependent PL data. The EMM provides excellent fits to the diameter-dependent data obtained at both room temperature and 7 K, and shows that the shifts in the emission spectra can be explained by radial quantum confinement.

Introduction

Nanocrystals (NCs)[1] and nanowires (NWs)[2] have attracted considerable attention due to the interesting fundamental properties present in such low-dimensional systems and the exciting prospects for utilizing these materials in nanotechnology-enabled electronic and photonic applications. For example, ensembles of NCs, which exhibit well understood size-dependent optical properties, have been used to fabricate light-emitting diodes (LEDs).[3] More recently, stimulated emission at wavelengths tunable by the NC diameter has also been demonstrated.[4] The development of nanoscale electrical and optoelectronic devices based on individual NCs has met with less success, however, due in part to the challenges associated with making electrical contacts to a single NC.[5]

On the other hand, the assembly of active nanoscale devices from individual NWs is relatively straightforward since NWs can function both as active elements and the "wires" carrying current to and from devices. For example, nanoscale field-effect transistors,[6−8] inverters,[7,8] and more complex logic gates[8] have been demonstrated using well-defined NW building blocks. In addition, LEDs[6] and photodetectors[9] have been assembled using NWs, and optically pumped lasing has been reported in NW arrays and individual NWs.[10] These results highlight the promise of bottom-up assembly of NWs, yet developing a fundamental understanding of the electrical and optical properties of NWs remains absolutely essential for defining future applications.

In the case of optical properties, most previous studies of one-dimensional nanostructures have focused primarily on lithographically and epitaxially defined quantum wires, such as "T-shaped" and "V-groove" quantum wires.[11−13] Quantum wires differ substantially from NWs since these wire-like nanostructures are embedded in a substrate of similar dielectric constant with a noncylindrical confining potential. In NWs, the potentials for electrons and holes are radially symmetric, and the surrounding medium (air or vacuum) has a considerably lower dielectric constant, which can introduce new and interesting physical properties.[14]

To explore the potentially unique optical properties of NW building blocks, herein we report studies of the size-dependent PL properties of InP NWs. PL images and spectra have been recorded on individual, isolated InP nanowires at both room temperature (RT) and 7 K. The PL images show that the emission intensity along the wire axis is relatively uniform within the experimental resolution, and spectra recorded at different positions along the wire give nearly identical line shapes and emission energies. Furthermore, PL spectra obtained from nanowires of varying diameters indicate that emission maxima systematically shift to higher energy with decreasing nanowire diameter. An effective mass model (EMM) using particle-in-a-cylinder wave functions for both electrons and holes has been used to analyze the observed size-dependent luminescence spectra.

Experimental Section

Nearly monodisperse, single-crystal InP NWs were grown via laser-assisted catalytic growth (LCG) using gold NC catalysts as described previously.[15−17] Briefly, 10, 15, 20, or 50 nm diameter gold NC solutions (BBI International) were dispersed on oxidized silicon substrates (600 nm thermal oxide, Silicon Sense), and then the substrates were placed at the downstream end of a quartz reactor. The reactor was heated to 650−700 °C in a flow of 100 standard cubic centimeters per minute (sccm) of argon, and then an InP target was ablated for 5−10 min using a Nd:YAG laser ($\lambda = 1064$ nm, 7 ns pulse, 20−30 Hz). NW samples were dispersed in ethanol via sonication, and then deposited onto quartz substrates for PL measurements. The structural characterization of the InP NWs has been described previously.[15,17]

Single NW PL images and spectra were obtained using a home-built epifluorescence microscope. NWs were excited with the 488 nm line from an argon-ion laser (Model 532, Melles Griot). The excitation light was reflected from a dichroic mirror and focused by an objective (Nikon, NA = 0.7) onto the quartz substrate with dispersed NWs. The typical excitation power

Letters

J. Phys. Chem. B, Vol. 106, No. 16, 2002 **4037**
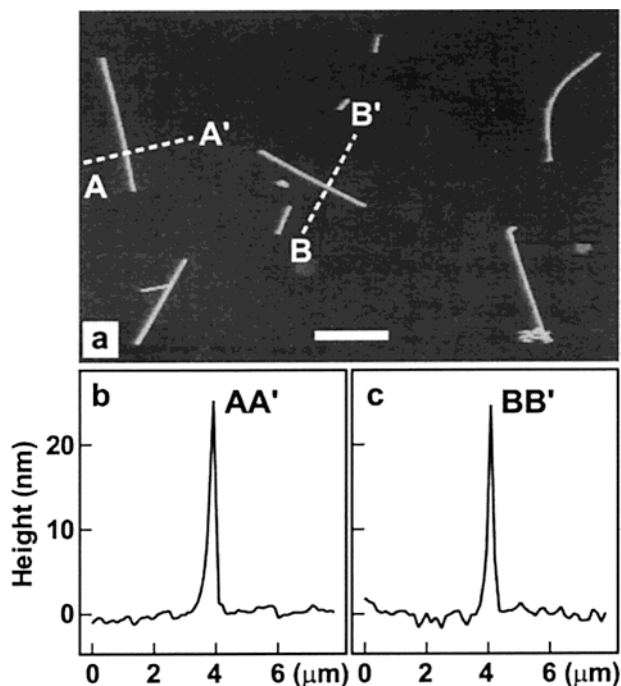
Figure 1. (a) Contact-mode AFM height image of InP nanowires dispersed on a quartz substrate. Scale bar is 5 μm. (b,c) Representative cross sections taken along the lines AA′ and BB′ in (a). The measured NW diameters in (b) and (c) are 25.3 and 24.6 nm, respectively.
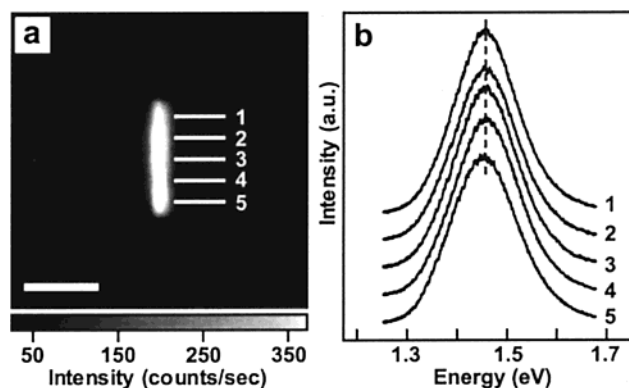

Figure 2. (a) Typical PL image recorded on an individual InP NW. Scale bar is 5 μm. (b) PL spectra taken at the positions indicated in (a). The spectra were shifted vertically for clarity. The PL image and spectra shown here were taken at RT from an ca. 15 nm diameter NW. The exposure times for the PL image and spectra were 2 and 10 s, respectively.
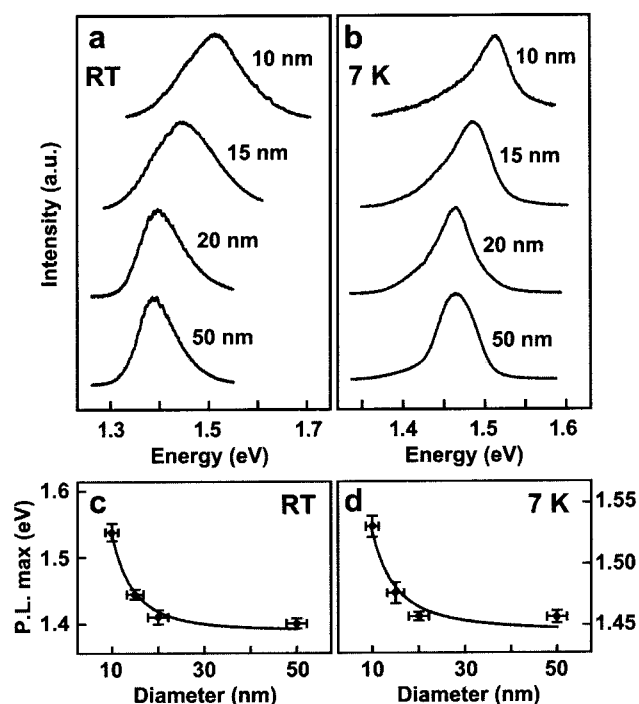
Figure 3. (a) PL spectra taken at RT from single InP NWs with nominal diameters of 50, 20, 15, and 10 nm. (b) Single NW PL spectra at 7 K. (c) Emission energy maxima at RT versus NW diameter. (d) Emission energy maximum at 7 K. PL spectra in (a) and (b) were normalized to the peak maxima and shifted upward for clarity. The experimental data in (c) and (d) were fit using the EMM (solid line) described in the text.

density was ~1 kW/cm². The quartz substrate was mounted in air for RT measurements or on the cold finger of a liquid helium cryostat for measurements at 7 K. PL was collected by the same objective, passed through a long-pass filter to remove excitation light, focused onto the entrance slit of a spectrometer, and either imaged or spectrally dispersed onto a liquid nitrogen cooled charge coupled device (CCD) (LN/CCD-512, Roper Scientific).

Results and Discussion

The InP NW samples dispersed on quartz were characterized by atomic force microscopy (AFM) imaging prior to our PL measurements (Figure 1). AFM images show that the samples consist of well-separated NWs, which enables the intrinsic PL properties of the individual NWs to be measured. In addition, cross-sections determined from AFM height images show that the distinct NWs in a given sample have nearly identical diameters (Figure 1b,c); these results are consistent with our transmission electron microscopy studies of NWs grown using gold NC catalysts.[16,17]

A typical PL image of a single InP NW recorded at room temperature is shown in Figure 2a. The recorded emission intensity is quite uniform (±5% variation) over the entire nanowire length within the ~1 μm spatial resolution of our experiments.[9] In addition, luminescence spectra obtained at different positions along the nanowire axis (Figure 2b) show nearly identical emission energies (less than 1% variation) and line shapes. Uniform PL is also observed in measurements recorded at low temperature (7 K). These results, which show uniform PL and little variation for a given diameter, indicate that the InP NWs are of good quality and can provide insight into size-dependent properties.

The InP NWs should exhibit size-dependent PL for diameters less than ca. the bulk exciton diameter, 19 nm,[18] due to quantum confinement. To address this fundamental issue directly, the PL spectra of nanowires with diameters of 50, 20, 15, and 10 nm were collected. Representative spectra recorded at RT (Figure

3a) and 7 K (Figure 3b) exhibit a systematic shift to higher energy as the nanowire diameters are reduced below 20 nm, in agreement with the concept of quantum confinement.[1a] In addition, these experiments show that all of the diameter-dependent spectra recorded at 7 K shift to higher energy, consistent with the shift of the bulk band gap from 1.35 to 1.42 eV as the temperature is reduced from RT to 7 K. For example, the emission energy of 15 nm diameter wires at RT is 1.45 eV, and shifts to 1.48 eV at 7 K.

The statistical significance of these diameter- and temperature-dependent data have been determined by analyzing measurements carried out on a number of independent NWs for each nominal diameter. We recorded PL data from 20 to 50 NWs for a given sample and used at least three independent samples

4038 *J. Phys. Chem. B, Vol. 106, No. 16, 2002*

Letters

for each diameter. Significantly, these data show virtually the same luminescence maxima and line shapes for each diameter and temperature. Plots summarizing the diameter dependent PL maxima determined at RT (Figure 3c) and 7 K (Figure 3d) from nominally 10, 15, 20 and 50 nm diameter NWs demonstrate that the uncertainty in emission energies between wires is small (~1%) compared to the substantial blue-shift in the emission maximum with decreasing diameter. These results also testify to the uniformity of these NWs.

To explore quantitatively the observed size-dependent nanowire luminescence, we compared these data to an effective mass model (EMM)[19] developed for a cylindrical potential for electrons and holes. In this model, particle-in-a-cylinder wave functions[20] are used for both electrons and holes:

$$\Psi(r_{e,h}, z_{e,h}) = N J_0\left(\alpha_{01}\frac{r_{e,h}}{R}\right) \sin\left(\pi\frac{z_{e,h}}{L}\right) \quad (1)$$

where $J_0(\alpha_{01}r_{e,h}/R)$ is the zeroth-order Bessel function, α_{01} the first zero of the zeroth-order Bessel function (2.405), L the length of the cylinder, and N the normalization constant. The calculated energy shift ΔE, relative to the bulk band gap as a function of the nanowire radius R, is given by[20]

$$\Delta E = \frac{\hbar^2}{2m^*}\left(\left(\frac{\alpha_{01}}{R}\right)^2 + \left(\frac{\pi}{L}\right)^2\right) - \left\langle \Psi(x_e)\Psi(x_h)\left|\frac{e^2}{\epsilon|x_e - x_h|}\right|\Psi(x_h)\Psi(x_e)\right\rangle \quad (2)$$

where m^* is the reduced effective exciton mass ($m_e m_h/(m_e + m_h)$), $\hbar$ is Planck's constant, e the electron charge, and ϵ the dielectric constant of InP. The first term in eq 2 represents the size-dependent kinetic energy confinement imposed by the walls of the nanowire cylinder. The second term is the attractive Coulomb interaction between electron and hole to first order in perturbation theory. The Coulomb interaction was numerically evaluated using the Green's function expansion in terms of Bessel functions:[20]

$$\frac{1}{|x_e - x_h|} = \sum_{m=-\infty}^{\infty} \int_0^\infty e^{im(\varphi_e - \varphi_h)} J_m(kr_e) J_m(kr_h) e^{-k|z_e - z_h|} \, dk \quad (3)$$

where $J_m(kr_{e,h})$ is the mth order Bessel function.

We find that our data are well fit by the EMM at RT (Figure 3c) and 7 K (Figure 3d) using the reduced effective mass m^* as the primary fitting parameter. The good fit of the experimental data suggests that this model captures the essential physics of the system. The reduced effective mass at RT determined from the fit, $0.052m_0$ (m_0, the free electron mass), is in reasonable agreement with the literature value of $0.065m_0$ (calculated using $m_e = 0.078$ and the geometric mean of the anisotropic hole masses, $m_h = 0.40$) for bulk InP.[21] Interestingly, the smaller effective mass determined from our data can be attributed to the crystalline orientation of the nanowires; that is, the $\langle 111 \rangle$ nanowire growth axis corresponds to the heavy hole direction in InP.[21] The smaller observed effective mass is thus consistent with confinement perpendicular to the growth direction, where the hole mass is reduced. The value of the reduced mass determined from the 7 K data, $0.082m_0$, is larger than the RT value but consistent with the observation that the effective carrier masses in InP increase with decreasing temperature within the accuracy of the known data.[22]

These data (Figure 3) also enable us to address other issues. First, we find that fits of the effective mass m^* to the data are
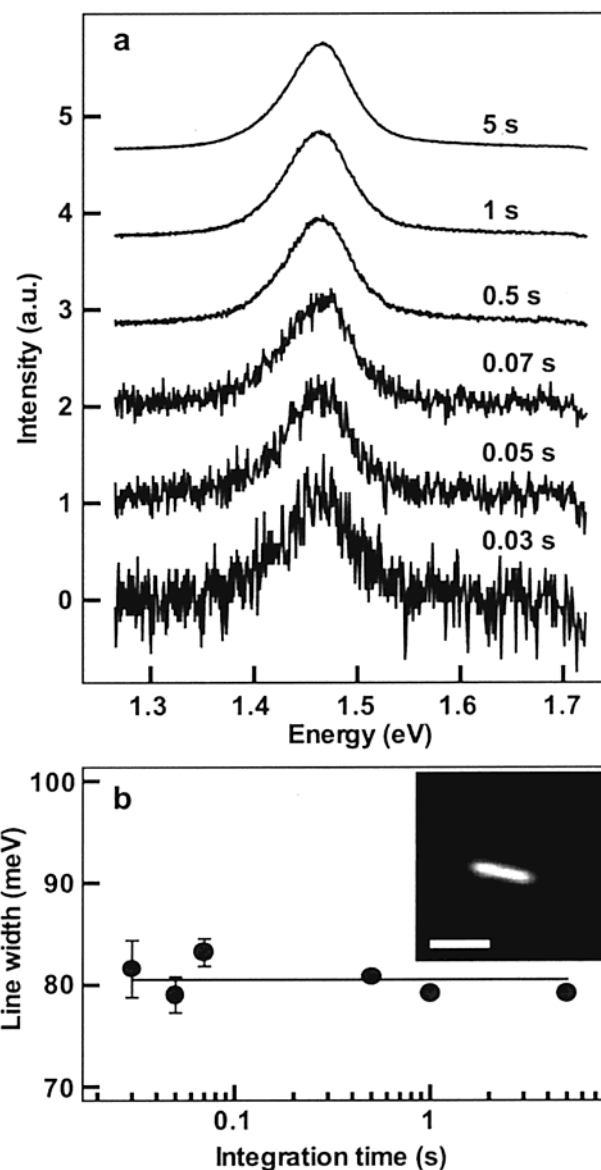
Figure 4. (a) PL spectra of a single InP nanowire recorded for different integration times. The spectra were normalized to the peak maximum and shifted vertically for clarity. (b) PL line width as a function of integration time obtained from the spectra in (a) using Gaussian fits. The solid line is an average of all the line width values. (inset) PL image of the 20 nm diameter NW characterized in (a); scale bar is 5 μm. The data were recorded at 7 K with a power density of ca. 1 kW/cm².

relatively insensitive to the value of L with reasonable fits obtained for $L > 10$ nm. Values of L less than the true nanowire length account phenomenologically for the slight blue shift in the PL present even in 50 nm nanowires. These large diameter wires are expected to be similar to bulk InP due to the fact that the diameter should impose no confinement on the excitons (bulk exciton diameter ≈ 20 nm). Further studies are underway to understand the origin of the slight shift of the emission energy of large diameter nanowires from the band gap of bulk InP.

Second, the line widths are consistently broad in these single NW PL measurements with values at RT and 7 K of 100−150 and 50−90 meV, respectively. In comparison, studies of embedded quantum wires have exhibited low-temperature line widths approximately an order of magnitude smaller than we find here.[12,13] Previous low-temperature PL studies of CdSe NCs suggest that apparently broad line widths can be attributed to

Letters

J. Phys. Chem. B, Vol. 106, No. 16, 2002 **4039**

spectral diffusion resulting from Stark shifts produced by changing local electric fields.[23] To investigate if spectral diffusion contributes to our broad single wire line widths, we measured PL spectra on single InP nanowires with integration times varying from 30 ms to 5 s at 7 K (Figure 4a). Significantly and in contrast to the CdSe NC work, the NW PL line widths show no dependence on integration time (Figure 4b). These results imply that either spectral diffusion occurs on a time scale faster than our 30 ms detection limit (and faster than in CdSe) or other effects dominate the line width. Comparison to recent data obtained on high-quality quantum wires[24] suggests that the widths might signify delocalization of excitons over extended distances. However, inhomogeneous broadening by surface states and small diameter fluctuations may also contribute to the observed NW line widths. Future experiments designed to address these interesting questions are currently in progress.

In conclusion, PL imaging and spectroscopy have been used to characterize the optical properties of isolated, individual InP NWs with diameters ranging from 10 to 50 nm at RT and 7 K. PL images and spectra show that the emission maxima, line shapes and intensities are nearly identical along the axis of a given NW, and PL spectra show that emission maxima systematically shift to higher energy with decreasing wire diameter, for diameters less than 20 nm. An EMM developed using particle-in-a-cylinder wave functions for electrons and holes was found to provide excellent fits to the diameter-dependent data obtained at both room temperature and 7 K, and shows that shifts in the emission spectra can be explained by radial quantum confinement. We believe that the ability to tune emission energy through diameter variations could lead to a number of exciting applications of these NWs. For example, the tunability of the InP NW optical properties and our ability to synthesize NWs of virtually any group III−V, or II−VI semiconductor material,[15] suggest that recently reported nanoscale LEDs[6] and polarization-sensitive photodetectors[9] could be assembled covering a broad spectral range. Last, the nanoscale dimensions of these NWs offer promise for producing highly integrated photonic circuits.

References and Notes

(1) (a) Alivisatos, A. P. *Science* **1996**, *271*, 933. (b) Murray, C. B.; Norris, D. J.; Bawendi, M. G. *J. Am. Chem. Soc.* **1993**, *115*, 8706.

(2) (a) Hu, J.; Odom, T. W.; Lieber, C. M. *Acc. Chem. Res.* **1999**, *32*, 435. (b) Lieber, C. M. *Solid State Commun.* **1998**, *107*, 607. (c) Lieber, C. M. *Sci. Am.* **2001**, Sept, 58.

(3) Colvin, V. L.; Schlamp, M. C.; Alivisatos, A. P. *Nature* **1994**, *370*, 354.

(4) Klimov, V. I.; Mikhailovsky, A. A.; Xu, S.; Malko, A.; Hollingsworth, J. A.; Leatherdale, C. A.; Eisler, H.-J.; Bawendi, M. G. *Science* **2000**, *290*, 314.

(5) Klein, D. L.; Roth, R.; Lim, A. K. L.; Alivisatos, A. P.; McEuen, P. L. *Nature* **1997**, *389*, 699.

(6) Duan, X.; Huang, Y.; Cui, Y.; Wang, J.; Lieber, C. M. *Nature* **2001**, *409*, 66.

(7) Cui, Y.; Lieber, C. M. *Science* **2001**, *291*, 851.

(8) Huang, Y.; Duan, X.; Cui, Y.; Lauhon, L. J.; Kim, K.-H.; Lieber, C. M. *Science* **2001**, *291*, 630.

(9) Wang, J.; Gudiksen, M. S.; Duan, X.; Cui, Y.; Lieber, C. M. *Science* **2001**, *293*, 1455.

(10) Huang, M. H.; Mao, S.; Feick, H.; Yan, H.; Wu, Y.; Kind, H.; Weber, E.; Russo, R.; Yang, P. *Science* **2001**, *292*, 1897; Johnson, J. C.; Yan, H. Q.; Schaller, R. D.; Haber, L. H.; Saykally, R. J.; Yang, P. D. *J. Phys. Chem. B* **2001**, *105*, 11387.

(11) Someya, T.; Akiyama, H.; Sakaki, H. *Phys. Rev. Lett.* **1995**, *74*, 3664.

(12) Vouilloz, F.; Oberli, D. Y.; Dupertuis, M.-A.; Gustafsson, A.; Reinhardt, F.; Kapon, E. *Phys. Rev. B* **1998**, *57*, 12378.

(13) Hasen, J.; Pfeiffer, L. N.; Pinczuk, A.; He, S.; West, K. W.; Dennis, B. S. *Nature* **1997**, *390*, 54.

(14) Goldoni, G.; Rossi, F.; Molinari, E. *Phys. Rev. Lett.* **1998**, *80*, 4995.

(15) Duan, X.; Lieber, C. M. *Adv. Mater.* **2000**, *12*, 298.

(16) Gudiksen, M. S.; Lieber, C. M. *J. Am. Chem. Soc.* **2000**, *122*, 8801.

(17) Gudiksen, M. S.; Wang, J.; Lieber, C. M. *J. Phys. Chem. B* **2001**, *105*, 4062.

(18) Ashcroft, N. W.; Mermin, N. D. *Solid State Physics*; Harcourt College Publishers: Orlando, 1976; pp 626−628.

(19) Brus, L. E. *J. Chem. Phys.* **1984**, *80*, 4403.

(20) Arfken, G. B.; Weber, H. J. *Mathematical Methods for Physicists*; Academic Press: San Diego, 1995.

(21) Fu, H.; Zunger, A. *Phys. Rev. B* **1997**, *55*, 1642.

(22) Schneider, D.; Rürup, D.; Schönfelder, B.; Schlachetzki, A. *Z. Phys. B* **1996**, *100*, 33.

(23) Empedocles, S. A.; Bawendi, M. G. *J. Phys. Chem. B* **1999**, *103*, 1826.

(24) Intonti, F.; Emiliani, V.; Lienau, C.; Elsaesser, T. *Phys. Rev. B* **2001**, *63*, 5313.